Lens Epithelium-Derived Growth Factor Is an Hsp70-2 Regulated Guardian of Lysosomal Stability in Human Cancer

Mads Daugaard,[1] Thomas Kirkegaard-Sørensen,[1] Marie Stampe Ostenfeld,[1] Mads Aaboe,[2] Maria Høyer-Hansen,[1] Torben Falck Ørntoft,[2] Mikkel Rohde,[1] and Marja Jäättelä[1]

[1]Apoptosis Department, Danish Centre for Translational Breast Cancer Research and Centre for Genotoxic Stress Research, Institute of Cancer Biology, Danish Cancer Society, Copenhagen, Denmark and [2]Department of Clinical Biochemistry, Aarhus University Hospital, Skejby, Aarhus, Denmark

Abstract

Heat shock protein 70-2 (Hsp70-2) is a chaperone protein essential for the growth of spermatocytes and cancer cells. Here, we show that Hsp70-2 depletion triggers lysosomal membrane permeabilization and cathepsin-dependent cell death and identify lens epithelium-derived growth factor (LEDGF) as an Hsp70-2–regulated guardian of lysosomal stability in human cancer. Knockdown of LEDGF in cancer cells induces destabilization of lysosomal membranes followed by caspase-independent and Bcl-2–resistant cell death. Accordingly, ectopic LEDGF stabilizes lysosomes and protects cancer cells against cytotoxicity induced by anticancer agents that trigger the lysosomal cell death pathway. Remarkably, ectopic LEDGF also increases the tumorigenic potential of human cancer cells in immunodeficient mice, and LEDGF expression is increased in human breast and bladder carcinomas correlating with that of Hsp70-2 in invasive bladder cancer. Taken together, these data reveal LEDGF as an oncogenic protein that controls a caspase-independent lysosomal cell death pathway. [Cancer Res 2007;67(6):2559–67]

Introduction

The human heat shock protein 70 (Hsp70) family consists of at least eight highly homologous members that differ from each other by intracellular localization and expression pattern (reviewed in refs. 1–3). Six of them (Hsp70-1A, Hsp70-1B, Hsp70-1L, Hsp70-2, Hsp70-6, and Hsc70) reside mainly in the cytosol, one localizes to the mitochondria (mtHsp70), and one to the endoplasmatic reticulum (Bip). Hsp70 family members function as ATP-dependent molecular chaperones that assist folding of newly synthesized polypeptides, assembly of multiprotein complexes, transport of proteins across cellular membranes, and targeting of proteins for lysosomal degradation. A long line of experimental evidence positions the major stress-inducible Hsp70 (Hsp70-1A/B; here referred to as Hsp70-1) as a cancer-associated survival protein with oncogenic potential (4–9). In addition, the highly homologous Hsp70-2 has recently been identified as a potential cancer-promoting protein expressed at high levels in a subset of human breast cancers (10). Apart from cancer, Hsp70-2 is expressed at high levels in the testis and at considerably lower or nondetectable levels in other tissues (11). It has been assigned a particular function in male germ cells, where it is essential for the formation of the active CDC2/cyclin B complex during the metaphase of the first meiotic division (12). Accordingly, male mice deficient of Hsp70-2 are sterile due to massive spermatocyte apoptosis (13). Depletion of Hsp70-2 in cancer cells induces G_1 arrest and senescence that are mediated by an up-regulation of the expression of macrophage inhibitory cytokine-1 (MIC-1; ref. 10). Interestingly, cancer cells depleted for Hsp70-1 and Hsp70-2 display strikingly different morphologies, cell cycle distributions, and gene expression profiles, indicating that in spite of their remarkable homology, Hsp70 family members either display specificity for their client proteins or serve chaperone-independent specific functions in cancer cells (10).

Most normal cells respond to death stimuli by undergoing caspase-dependent apoptosis. In contrast, cancer cells frequently escape spontaneous and therapy-induced caspase activation due to acquired mutations in their apoptotic machinery (14, 15). For example, up-regulation of antiapoptotic Bcl-2 family members and mutations in p53 tumor suppressor protein are common in human tumors. Apoptosis-resistant cancer cells are, however, not completely resistant to cell death, but can die via alternative cell death pathways often involving noncaspase proteases such as cathepsins and calpains (16–18). Emerging evidence also suggests that the alternative cell death pathways can be selected during tumor development. For example, the levels of cytosolic inhibitors or lysosomal proteases are commonly increased in cancer cells and tissues (19–21), and Hsp70-1 is found in the endolysosomal membranes of many tumor cells and stressed cells where it inhibits the release of lysosomal cathepsins into the cytosol (22, 23). Thus, better knowledge of tumor-associated proteins that control alternative cell death pathways is of great importance for the understanding of drug resistance and development of more effective cancer therapies.

This study was initiated by data showing that Hsp70-2–depleted cancer cells undergo MIC-1–independent cell death. To identify the Hsp70-2–regulated protein(s) responsible for the cell death phenotype, we chose potential candidates among the genes found to be regulated by Hsp70-2 depletion in HeLa cervix carcinoma cells by Affymetrix genechip microarray analysis and investigated their effect on cell survival. This analysis revealed that the down-regulation of lens epithelium-derived growth factor (LEDGF; also known as p75, PC4, and SFRS1 interacting protein 2 and dense fine speckles 70) is responsible for the death of Hsp70-2–depleted cancer cells, and that LEDGF possesses great oncogenic potential. Thus, we studied the survival function of LEDGF in further detail and analyzed its expression in large panels of tissue biopsies originating from human bladder, colon and breast cancers, and their

Note: Present address for M. Aaboe: Cold Spring Harbor Laboratory, Cold Spring Harbor, NY 11724.

M. Rohde and M. Jäättelä share the senior authorship.

Requests for reprints: Marja Jäättelä, Apoptosis Department, Institute for Cancer Biology, Danish Cancer Society, Strandboulevarden 49, DK-2100 Copenhagen, Denmark. Phone: 45-35257318; Fax: 45-35257721; E-mail: mj@cancer.dk.

doi:10.1158/0008-5472.CAN-06-4121

corresponding normal tissues. Our data identify LEDGF as a cancer-associated survival protein that inhibits a caspase-independent lysosomal cell death pathway.

Materials and Methods

Cell culture. MCF-7 breast carcinoma, HeLa cervix carcinoma, U2OS osteosarcoma, WI-38 lung fibroblast, MCF-10A mammary epithelial, HBL-100 mammary epithelial, and PNT1A prostate epithelial cells, as well as single cell clones of MCF-7 cells transfected with an empty pCEP-4 vector (Invitrogen, Carlsbad, CA) or pCEP-4 encoding for human Bcl-2 (24), or with a plasmid encoding for a fusion protein consisting of enhanced green fluorescent protein and rat microtubule-associated protein-1 light chain-3 (eGFP-LC3; ref. 25), were grown in RPMI 1640 with Glutamax-1 (Invitrogen) supplemented with 6% FCS (Biological Industries) and antibiotics. The growth medium for MCF-10A cells was further supplemented with additional FCS (10% final concentration), 500 ng/mL hydrocortisone (Sigma, St. Louis, MO), 100 ng/mL cholera toxin (Sigma-Adlrich), 20 ng/mL epidermal growth factor, and 100 ng/mL insulin, and that of MCF-7 transfectants with appropriate antibiotics. The cells were maintained in a humidified atmosphere (37°C, 5% CO_2, 21% O_2) and regularly tested and found negative for *Mycoplasma*.

Siramesine was kindly provided by Christian Thomsen (Lundbeck A/S, Valby, Denmark), CRA12529 by Bob Rydzewski (Celera, South San Francisco, CA), and tumor necrosis factor (TNF) by Anthony Cerami (Kenneth Warren Laboratories, Tarrytown, NY). Etoposide, doxorubicin, and staurosporine were from Sigma, and zVAD-fmk was from Bachem (Bubendorf, Switzerland).

Transfections. Small interfering RNAs (siRNA) targeting *HSPA1A* and *HSPA1B* (A1), *HSPA2* (A2.1, A2.2, and A2.3), *HSPA6* (A6); *HSPA8* (A8), *HSPA1L* (A1L), *MIC-1* (M1), and a control siRNA (C) were described previously (10). SiRNAs against *LEDGF*, 5′-gcaaugaggaugugacuaa-3′ (L1), and 5′-gguaaucagc-cacaacaua-3′ (L2) were from Dharmacon Research (Lafayette, CO). HeLa, MCF-7, HBL-100, and U2OS cells were transfected with OligofectAMINE (Invitrogen) and MCF-10A, PNT1A, and WI-38 with ExtremeGene siRNA Transfection agent (Roche, Basel, Switzerland) according to the manufacturer's guidelines and with 50 nmol/L siRNA.

LEDGF cDNA was isolated by reverse transcription-PCR (RT-PCR) from HeLa cells and inserted between *Eco*R1 and *Hin*dIII sites in pcDNA3.1 (Invitrogen) creating pcDNA-LEDGF. pcDNA-LEDGF* was created by introducing three silent mutations (bold) in the target sequence of the L2 siRNA by PCR using 5′-ctgatgctcaagatgg**a**aatca**a**ccacaaca**c**aacggggagagca-3′ and its complementary sequence. pcDNA-Hsp70-2* with two silent mutations in the target sequence of A2.2 siRNA was described previously (10). When indicated, the transfected cells were visualized by cotransfection (1:6) of pEGFP-N1 (Clontech, Mountain View, CA). Plasmid transfections were done with Fugene HD (Roche) according to standard protocol. Cotransfections with plasmid and siRNA were done by transfecting the siRNA 24 h after the plasmid.

Primary tissue samples. Complementary DNA samples for RT-PCR analysis of human breast tissue (normal, primary tumor, and metastasis) were kindly provided by Per Thor Straten and Per Guldberg (Department of Tumor Cell Biology, Danish Cancer Society, Denmark). All tissue samples were obtained from patients operated at the Copenhagen University Hospital and assigned to a research program under the administration of the Danish Centre for Translational Breast Cancer Research. Bladder biopsies were obtained at the Aarhus University Hospital in Denmark and colon biopsies at 15 different clinics in Denmark and Finland. Tissues were frozen immediately in a preserving solution of guanidinium thiocyanate and stored at −80°C. Informed consent was obtained in all cases, and protocols were approved by the local scientific ethical committee.

Analysis of mRNA. RNA was harvested from HeLa cell culture or homogenized primary tissue and analyzed by RT-PCR as described previously (10). HeLa cDNA was used as template in a duplex PCR reaction performing the amplification (20 cycles) of LEDGF and the housekeeping gene porphobilinogen deaminase (PBGD). Primers in 5′-3′ directions were gcagcctaagaaggatgaag + gagcttgttgcattgtgacc and catgtctggtaacggcaatg + agggcatgttcaagctcctt, respectively. The samples were separated by gel electrophoresis (1% agarose containing 50 μg/mL ethidium bromide). The gels were scanned, and bands were quantified with the Image Gauge software (Fujifilm) in Quant mode as ImageGaugeQuant (IGQ) = $(\text{volume}_{\text{band}} - \text{volume}_{\text{background}})/\text{area}_{\text{pixels}}$. The expression of genes was computed as the fraction IGQ_{LEDGF}/IGQ_{PBGD}. The cDNA synthesized from the breast biopsies was analyzed by a real-time PCR done in the LightCycler 2.0 (Roche) with the FastStart SYBR-green I Master-mix (Roche) and the following primers in 5′-3′: caggtcacaatgcaacaagc and cttgggtgat-cacggaatct for *LEDGF* and tccaagcggagccatgtctg and agaatcttgtcccctgtgga for *PBGD* at 500 nmol/L as described (10). The *LEDGF* expression in each tissue sample was normalized to an external standard curve and evaluated relative to the *PBGD* expression.

Affymetrix microarray analyses on HeLa cells depleted of Hsp70-1 or Hsp70-2 as well as on bladder and colon biopsies were published previously (10, 26–29). Data were normalized either using the guanine cytosine content adjusted-robust multiarray (GC-RMA) procedure (HG-U133A; ref. 30) or by procedures for customized Affymetrix microarrays (Eos Hu03; ref. 31).

Immunoblotting. Primary antibodies used included murine monoclonal antibodies against LEDGF (Clone 26, BD Biosciences PharMingen, San Diego, CA), Hsp70 (2H9; kindly provided by Boris Margulis, Russian Academy of Sciences, St. Petersburg, Russia), glyceraldehyde-3-phosphate dehydrogenase (GAPDH, Biogenesis, Poole, United Kingdom) and β-tubulin (Biogenesis), goat antiserum against MIC-1 (Santa Cruz Biotechnology, Santa Cruz, CA), and rabbit antiserum 789 against Hsp70-2 (10). Immunodetection of proteins separated by 10% to 12% SDS-PAGE and transferred to nitrocellulose was done using appropriate peroxidase-conjugated secondary antibodies from DAKO A/S (Glostrup, Denmark), enhanced chemiluminescence Western blotting reagents (Amersham, GE Healthcare, Buckinghamshire, United Kingdom) and Luminescent Image Reader (LAS-1000Plus, Fujifilm Denmark, Vedbaek, Denmark).

Analysis of cell density, cell death, autophagy, and morphology. Cell density was assessed by the 3-(4,5-dimethylthiazol-2-yl)-2,5-diphenyltetrazolium bromide (MTT; Sigma-Aldrich) reduction assay and cell death by lactate dehydrogenase (LDH) release assay (Roche) essentially as described previously (32).

Apoptosis like cell death was assessed by staining the cells with 2.5 μg/mL Hoechst 33342 (Molecular Probes, Invitrogen) and counting cells with condensed nuclei in an inverted Olympus (Center Valley, PA) IX-70 fluorescent microscope (Filter U-MWU, 330–385 nm) connected to an Olympus C-3030 digital camera. For each experiment, a minimum of six randomly chosen areas with a minimum of 30 cells each were counted. Phase-contrast pictures of the cells were obtained with the same microscope.

Autophagy was detected in MCF7-eGFP-LC3 cells fixed in 3.7% formaldehyde and 0.19% picric acid (v/v) by counting the percentage of cells with a minimum of five eGFP-LC3–positve dots (a minimum of 2×100 cells per sample) applying Zeiss Axiovert 100M confocal laser scanning microscope (Carl Zeiss, Göttingen, Germany).

Enzymatic activity measurements. The effector caspase and cysteine cathepsin activities in cell lysates and cytosolic extracts from digitonin-treated cells were estimated using Ac-DEVD-7-amino-trifluoromethylcoumarin (AFC; BIOMOL Research Laboratories, Inc., Plymouth Meeting, PA) and zFR-AFC (Enzyme System Products, Livermore, CA) probes, respectively, as described previously (32). Protease activities were normalized to lactate dehydrogenase activity determined by a cytotoxicity detection kit (Roche).

Assay for the lysosomal pH. Cells incubated with the 2 μg/mL acridine orange (Molecular Probes) for 15 min at 37°C were washed in HBSS complemented with 3% FCS and analyzed at 37°C on an Axiovert 100M microscope equipped with the LSM510 laser scanning module for the red staining intensity in the lysosomes (areas with higher staining intensity than the background). The average staining intensity per pixel was defined in five areas containing 10 to 15 cells per sample using the LSM software (Carl Zeiss MicroImaging, Inc.).

Assay for lysosomal stability. Cells homogenized by 150 strokes in a DUALL glass homogenizer in a sucrose buffer [0.25 mol/L sucrose, 1 mmol/L EDTA, 20 mmol/L HEPES-NaOH (pH, 7.4)] were centrifuged at $1,000 \times g$ for 10 min, the supernatant was collected and centrifuged at $3,000 \times g$ for 10 min, and the resulting supernatant was centrifuged at $17,000 \times g$

for 10 min to obtain the light membrane fraction containing the majority of the lysosomes. The light membrane fractions were incubated in an isotonic (265 mOsm) or hypotonic (50–100 mOsm) sucrose buffer for 45 min on ice. The cysteine cathepsin (zFRase) activity in the supernatants was measured as described above, and the results are expressed as the percent of total activity released by 400 μg/mL digitonin.

Tumor xenografts. Single cell-cloned HeLa cells expressing either empty vector pcDNA3.1 (Invitrogen) or LEDGF (1.5×10^6 in 200 μL PBS) were inoculated s.c. into the right flank of female FOX CHASE severe combined immunodeficiency (SCID) mice. The tumor diameter was measured using a caliper, and the tumor volume was estimated according to the formula, $V = 4/3 \times \pi \times r^3$. All experiments were terminated at the time when the tumors in untreated animals reached maximum tolerated size ($r = 6$ mm). All animal work was carried out in accordance with the NIH guidelines.

Statistical analysis. Statistical significance was evaluated by two-sided paired Student's *t* test, and correlation was by Pearson's product moment test.

Results

Down-regulation of LEDGF mediates cell death in Hsp70-2–depleted cancer cells. We have recently shown that siRNA–mediated depletion of Hsp70-2 induces a substantial up-regulation of MIC-1 and MIC-1–dependent G_1 arrest in cancer cells (10). Here, we show that Hsp70-2 depletion induces a delayed MIC-1–independent cell death with apoptosislike chromatin condensation (Fig. 1). As we have shown earlier, the flat senescent phenotype of Hsp70-2–depleted cells was abolished by the codepletion of MIC-1, but the MIC depletion failed to rescue the cells from cell death occurring 72 to 96 h after the transfection. Prompted by the ability of several Hsp70-2 siRNAs to induce a similar apoptosislike phenotype (data not shown), we searched for putative Hsp70-2–regulated gene(s) responsible for the cell death phenotype. Affymetrix genechip analysis (10) revealed that the mRNA encoding for LEDGF, a protein reported to protect lens epithelial cells, keratinocytes, and fibroblasts from various stresses (33, 34), was 4.5-fold down-regulated in HeLa cells depleted for Hsp70-2 as compared with the control siRNA-treated cells (Fig. 2*A*). These data were confirmed by RT-PCR and immunoblot analyses of the siRNA-treated HeLa cells (Fig. 2*A* and *B*). The effective down-regulation of LEDGF protein in HeLa cells treated with three nonoverlapping Hsp70-2 siRNAs strongly suggested that the down-regulation of LEDGF was a specific consequence of Hsp70-2 depletion (Fig. 2*B*). Accordingly, ectopic Hsp70-2 containing two silent mutations in the sequence recognized by the A2.2 siRNA (Hsp70-2*) inhibited the A2.2-mediated down-regulation of LEDGF (Fig. 2*B*). Moreover, ectopic Hsp70-2 enhanced the expression of LEDGF in control cells further supporting the role of Hsp70-2 as a positive regulator of LEDGF expression (Fig. 2*B*). Interestingly, this regulatory effect was specific for Hsp70-2 because the depletion of

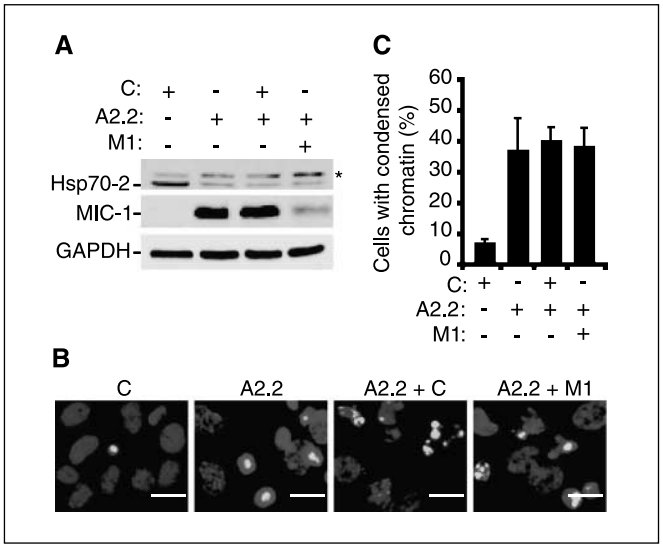

Figure 1. Depletion of Hsp70-2 induces MIC-1–independent apoptosislike cell death. HeLa cells were transfected with the control (*C*), Hsp70-2 (*A2.2*), and MIC-1 (*M1*) siRNAs in indicated combinations and analyzed 96 h later for the expression of Hsp70-2, MIC-1, and GAPDH (loading control) by immunoblotting (*A*) and for apoptosislike chromatin condensation by Hoechst 33342 staining and microscopy (*B* and *C*). A minimum of 6 × 30 cells were counted for each experiment. *C, columns,* means of three independent experiments; *bars,* SD. *B, bar*, 20 μm.

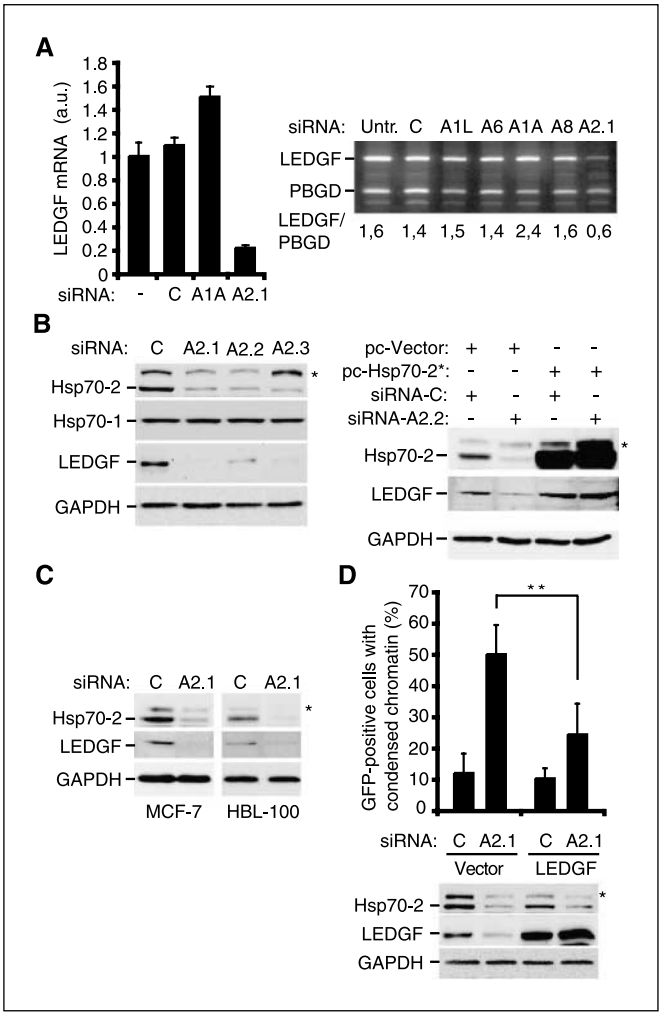

Figure 2. Cell death induced by Hsp70-2 depletion is mediated by LEDGF down-regulation. HeLa (*A* and *B*), MCF-7, and HBL-100 (*C*) cells were transfected with indicated siRNAs (*C*, control; *A1A*, Hsp70; *A2.1, A2.2*, and *A2.3*, Hsp70-2; *A1L*, Hsp70-1L; *A6*, Hsp70-6; *A8*, Hsc70) or plasmids and analyzed for the expression of the indicated mRNAs by Affymetrix genechip array (*A, left*) or RT-PCR (*A, right*) and proteins by immunoblotting (*B* and *C*) 48 and 84 h after the transfection, respectively. The values in (*A, left*) are arbitrary units normalized to the untreated cells; *columns,* means of two independent chip sets (four combinations); *bars,* SD. Hsp70-2* encodes for Hsp70-2 with two silent mutations in the sequence recognized by A2.2 siRNA. *, an unspecific band detected by the Hsp70-2 antiserum. *D,* HeLa cells were cotransfected with pEGFP-N1 and indicated plasmids and siRNAs 96 h before the analysis of apoptosislike chromatin condensation. A minimum of 6 × 30 green cells per experiment were counted. *Columns,* means of three independent experiments; *bars,* SD. **, *P* value <0.01.

highly homologous cytosolic Hsp70 family members (Hsp70-1, Hsp70-1L, Hsp70-6, and Hsc70) did not down-regulate LEDGF mRNA (Fig. 2*A*). The LEDGF expression depended on the Hsp70-2 also in MCF-7 breast cancer cells and in HBL-100 breast epithelial cells, suggesting that Hsp70-2 is a general regulator of LEDGF expression levels (Fig. 2*C*). Importantly, the ectopic expression of LEDGF effectively inhibited the cell death induced by Hsp70-2 depletion (Fig. 2*D*). Thus, Hsp70-2 and LEDGF are coregulated, and the down-regulation of LEDGF is an essential mediator of the cell death induced by Hsp70-2 depletion.

Depletion of LEDGF triggers lysosomal cell death pathway in cancer cells. To test whether the down-regulation of LEDGF is sufficient to induce cell death, we designed two nonoverlapping siRNAs (L1 and L2) that effectively inhibited the expression of LEDGF in various cell types (Fig. 3). LEDGF depletion decreased the density of HeLa cells in a time-dependent manner resulting in 60% to 65% reduction 4 days after the transfection (Fig. 3*A*). The reduced cell density was not associated with the G_1 cell cycle arrest or senescentlike flat phenotype characteristic of Hsp70-2–depleted HeLa cells (Fig. 3*B* and data not shown). Instead, the microscopic analysis revealed increasing numbers of detached rounded cells and apoptosislike chromatin condensation in over half of the cells 4 days after the transfection (Fig. 3*B*). The increase in cell death was further evidenced by the loss of plasma membrane integrity as shown by the release of a cytosolic enzyme (LDH) into the supernatant 3 days after the transfection (Fig. 3*B*). Notably, ectopic LEDGF cDNA with three silent mutations in the sequence recognized by the L2 siRNA (LEDGF*) reversed the cell death phenotype induced by the L2 but not the L1 siRNA (Fig. 3*C*). Correspondingly, ectopic wild-type LEDGF that was effectively silenced by the siRNAs failed to confer any rescue. Thus, the observed cell death phenotype was a specific consequence of LEDGF depletion. A similar phenotype was observed in LEDGF-depleted breast cancer (MCF-7) and osteosarcoma (U2OS) cells that detached and rounded up 2 to 4 days after the transfection, resulting in a dramatically reduced cell density, whereas the immortalized epithelial cells (HBL-100 and MCF-10A breast epithelium and PNT1A prostate epithelium) and primary lung

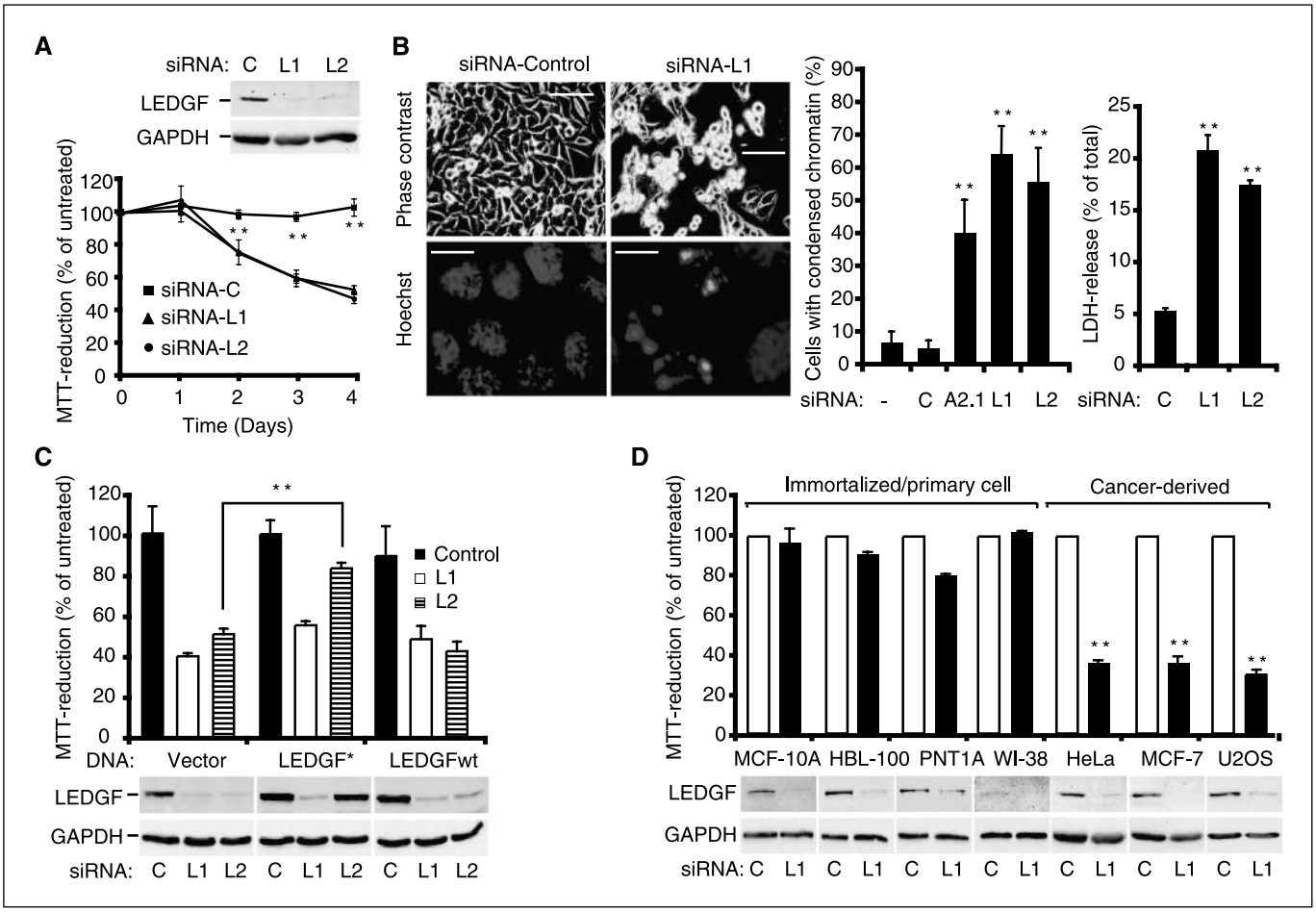

Figure 3. Depletion of LEDGF induces apoptosislike cell death in cancer cells. *A,* HeLa cells transfected with control siRNA or two nonoverlapping siRNAs against LEDGF (*L1* and *L2*) were analyzed for the expression of LEDGF and GAPDH by immunoblotting 72 h posttransfection and for cell density by MTT reduction assay 1 to 4 days after the transfection. The data are presented as percentage of MTT reduction in untreated cultures. *Points,* means of three triplicate experiments; *bars,* SD. *B,* HeLa cells were transfected with the indicated siRNAs and analyzed for the plasma membrane integrity by the LDH release assay (72 h) and the apoptosislike nuclear condensation by microscopy (96 h). *Columns,* means of three (LDH assay) or four (nuclear condensation) independent experiments; *bars,* SD. *Bar*, 80 μm (*top*) and 20 μm (*bottom*). *C,* HeLa cells transfected with an empty vector or cDNAs encoding for or wild-type LEDGF (*LEDGFwt*) or LEDGF with three silent mutations in the sequence corresponding to the LI siRNA sequence (*LEDGF**) and the indicated siRNAs were analyzed for cell density by MTT assay 96 h after the plasmid transfection. The data are presented as percentage of MTT reduction in untreated cultures. *Columns,* means of three triplicate experiments; *bars,* SD. *D,* the indicated cell lines were transfected with the control or LEDGF siRNA and analyzed 96 h later for cell density by MTT assay. The data are presented as percentage of MTT reduction in untreated cultures. *Columns,* means of three triplicate experiments; *bars,* SD. **, *P* value <0.01 as compared with cells transfected with either L1 or L2 (*A*), control siRNA (*B* and *D*) or vector (*C*).

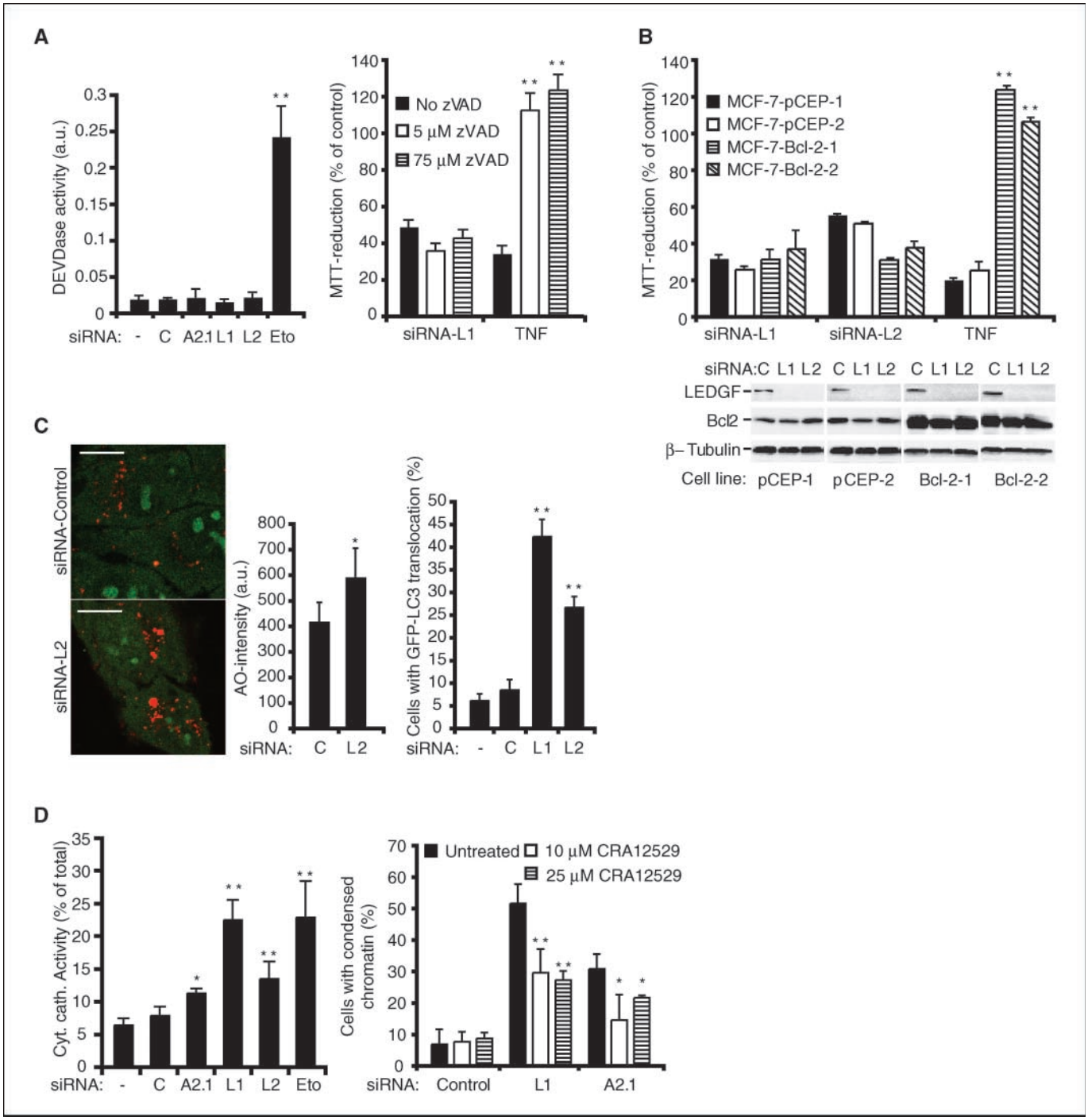

Figure 4. Knockdown of LEDGF induces cathepsin-dependent cell death that bypasses the Bcl-2 checkpoint. *A,* HeLa cells treated with a control, Hsp70-2, or LEDGF siRNAs for 72 h or with 50 μmol/L etoposide for 24 h were analyzed for effector caspase (*DEVDase*) activity (*left*). The values are represented as arbitrary units. *Columns,* means of three independent triplicate experiments; *bars,* SD. MCF-7 cells treated with LEDGF siRNA for 96 h or with 5 ng/mL TNF for 24 h were analyzed for cell density by MTT reduction assay (*right*). When indicated, zVAD-fmk was added to the cultures at the final concentration of 5 or 75 μmol/L 48 h before the analysis. The data are presented as percentage of MTT reduction in untreated cultures. *Columns,* means of three independent triplicate experiments; *bars,* SD. *B,* single cell clones of MCF-7 cells transfected with an empty pCEP vector (*pCEP-1* and *pCEP-2*) or pCEP encoding for Bcl-2 (*Bcl-2-1* and *Bcl-2-2*) were treated with indicated siRNAs for 96 h or with 5 ng/mL TNF for 24 h and analyzed for the indicated proteins by immunoblotting and for cell density by MTT reduction assay. The data are presented as percentage of MTT reduction in untreated cultures. *Columns,* means of three independent triplicate experiments; *bars,* SD. *C,* HeLa cells were treated with a control or LEDGF siRNA for 48 h and stained with acridine orange (*AO*). The intensity of the red staining was analyzed as described in Materials and Methods. Representative confocal images (*bar,* 20 μmol/L) and histograms with average red staining intensity (AO) per pixel are shown. MCF7-eGFP-LC3 were treated with olicofectamine alone (−) or with control or LEDGF siRNAs for 72 h, fixed and analyzed for the translocation of LC3 to vesicular structures (autophagosomes) by confocal microscopy. Histograms with percentages of green cellular cross-sections with over five LC3 positive dots are shown (*right*). *Columns,* means for three independent duplicate experiments; *bars,* SD. *D,* HeLa cells treated with a control, Hsp70-2, or LEDGF siRNA for 72 h or with 50 μmol/L etoposide for 24 h were analyzed for the cytosolic and total cysteine cathepsin activities (*left*). The values for the cytosolic cysteine cathepsin activity are presented as percentages of the total activity. The same cells were analyzed 96 h later for apoptosislike nuclear condensation (*right*). When indicated, cathepsin B inhibitor (*CRA12529*) was added at indicated concentrations. *Columns,* means of three independent experiments; *bars,* SD. *, *P* value <0.05; **, *P* value <0.01 as compared with the cells transfected with a control siRNA (*A, left*; *C*; and *D, left*) or with a vector (*B*), or with the cells without zVAD-fmk (*A, right*) or CRA12529 (*D, right*).

fibroblasts (WI-38) retained their adherent phenotype and cell density upon LEDGF depletion (Fig. 3*D* and data not shown).

The massive cell death in cancer cells depleted for LEDGF was not associated with a measurable effector caspase activity, and the potent pan-caspase inhibitor zVAD-fmk failed to inhibit the cell death in both HeLa and MCF-7 cells (Fig. 4*A* and data not shown). Furthermore, the cell death induced by LEDGF depletion was completely resistant to the antiapoptotic protein Bcl-2 that effectively inhibited TNF-induced apoptosis in MCF-7 cells (Fig. 4*B*). These data indicate that LEDGF depletion triggers a cell death pathway clearly distinct of classic cytochrome *c*– and caspase-mediated apoptosis. Thus, we investigated whether the LEDGF depletion induced a lysosomal cell death pathway characterized by an early increase in the volume of the acidic (lysosomal) compartment, permeabilization of lysosomes, and cathepsin-mediated execution (18, 35). Indeed, the cells depleted for LEDGF for 48 h displayed enhanced accumulation of acridine orange (an acidotropic and metachromatic weak base that emits red fluorescence when in high concentration), indicative of an increase of the volume of the acidic compartment of the cell (Fig. 4*C*). One day later (72 h after the siRNA transfection), LEDGF-depleted cells manifested with an increase in the number of autophagosomes (LC3-postive vesicles) and the destabilization of the lysosomes as shown by an increase in the cytosolic cysteine cathepsin activity (Fig. 4*C* and *D*). The lysosomal leakage was at least partially responsible for the cell death because a cell-permeable inhibitor of cathepsin B (CRA12529) conferred significant protection (Fig. 4*D*). Notably, the Hsp70-2 depletion induced a similar, albeit weaker, lysosomal leakage accompanied by cathepsin-dependent and caspase-independent cell death (Fig. 4*A* and *D*).

LEDGF enhances lysosomal stability, resistance to lysosome-targeting drugs, and tumorigenic potential of cancer cells. To further investigate the effects of LEDGF on cancer cell lysosomes, we created single cell clones of MCF-7 and HeLa cells that express ectopic LEDGF (Fig. 5*A*). The lysosomes isolated from the cells expressing ectopic LEDGF were significantly more resistant to an

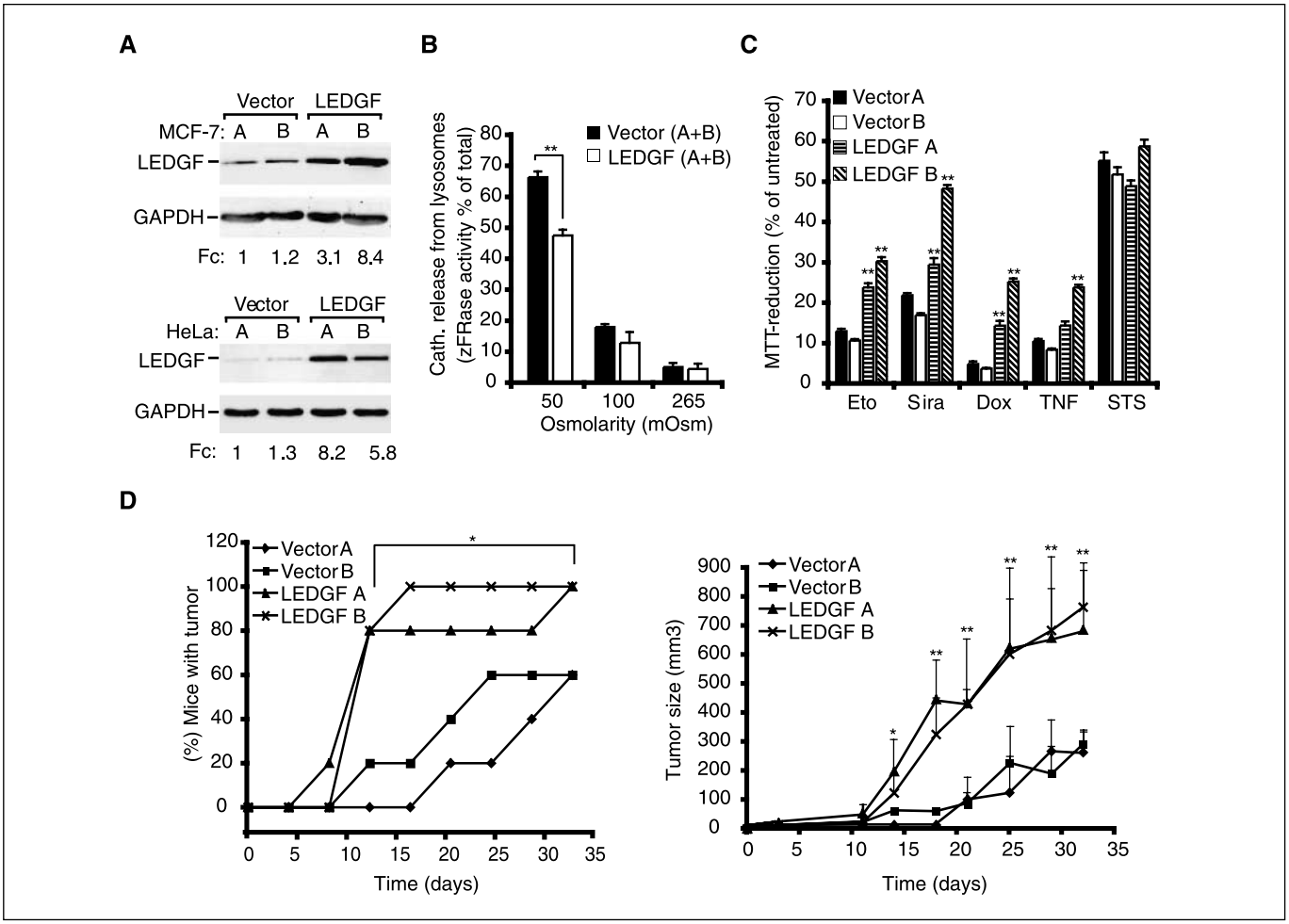

Figure 5. LEDGF induces resistance to the lysosomal cell death pathway and enhances tumorigenecity. *A,* stable single cell clones of MCF-7 and HeLa cells transfected with an empty vector or human LEDGF were analyzed for the expression of LEDGF and GAPDH by immunoblotting. *B,* the stability of lysosomes isolated from indicated MCF-7 transfectants was analyzed *in vitro* by incubating them for 45 min in isotonic (265 mOsm) and hypotonic (50–100 mOsm) conditions. The data are presented as percentage of cysteine cathepsin activity released to the supernatant. *Columns,* means of two independent duplicate experiments; *bars,* SD. *C,* the indicated MCF-7 transfectants were treated with 100 μmol/L etoposide (*Eto*), 4 μmol/L siramesine (*Sira*), 5 μmol/L doxorubicin (*Dox*), 5 ng/mL TNF or 100 nmol/L staurosporine (*STS*) for 24 h and analyzed for cell density by MTT reduction assay. The data are presented as percentage of MTT reduction in untreated cultures. *Columns,* means of three independent triplicate experiments; *bars,* SD. *D,* the indicated HeLa transfectants (1.5×10^6 per mouse, $n = 5$) were inoculated s.c. into SCID mice, and the tumor growth was followed for 33 days. The data indicate the percentage of mice with a measurable tumor ($r > 2.5$ mm; *left*). *Points,* mean tumor volume in tumor-bearing mice; *bars,* SD (*right*). *, *P* value <0.05; **, *P* value <0.01 when LEDGF-transfected cells are compared with either one of the vector-transfected cells (*B* and *C*) or when either one of LEDGF/75-transfected clones is compared with either one of vector-transfected clones (*D*).

in vitro exposure to hypotonic stress than those originating from vector-transfected control cells (Fig. 5*B*). Thus, LEDGF is likely to affect the stability of lysosomes instead of inhibiting a specific signaling pathway that leads to the lysosomal membrane permeabilization. Accordingly, the ectopic LEDGF protected MCF-7 cells against the cell death induced by various agents that trigger the lysosomal membrane permeabilization, i.e., siramesine, etoposide, doxorubicin, and TNF, whereas no protective effect was detected against a classic apoptosis inducer staurosporine (Fig. 5*C*; refs. 22, 24). The protection against cytotoxic drugs was dose dependent, the clone B (8.4-fold increase in the LEDGF expression) showing more pronounced drug resistance than the clone A (3.1-fold increase in the LEDGF expression). Moreover, the LEDGF-expressing MCF-7 clone B showed a tendency for an increased tumorigenic potential in an orthotopic breast cancer model in immunodeficient mice (data not shown). Even stronger enhancement of tumorigenecity was observed in a s.c. HeLa xenograft model, in which two single cell clones expressing ectopic LEDGF formed significantly more and significantly faster growing tumors than the two control clones (Fig. 5*D*).

Expression of LEDGF is increased in human breast and bladder cancer. We have earlier shown that the Hsp70-2 mRNA levels are elevated in a subset of primary and metastatic breast cancers (10). Prompted by our data showing that LEDGF is a potent survival factor that enhances tumorigenecity and that its expression is regulated by Hsp70-2 in cell culture, we next analyzed whether LEDGF expression is increased in human cancer tissues. The analysis of 80 breast biopsies originating from normal tissue (n = 11), primary carcinoma (n = 38), or metastatic carcinoma (n = 21) revealed that subpopulations of both primary tumors and metastases had higher LEDGF mRNA levels than the normal breast tissue (Fig. 6*A*). Furthermore, an analysis of microarray data on 90 bladder biopsies showed a significant increase in LEDGF mRNA expression in carcinomas invaded to the muscle (T2-4) as compared with the normal tissue as well as in both T2-4 carcinomas, and carcinomas invaded to the subepithelium and/or connective tissue (T1) as compared with the benign tumors (Fig. 6*B*). An additional analysis of 117 bladder biopsies by customized Affymetrix microarray platform Eos HU03 (36) supported the conclusion that LEDGF mRNA is elevated during bladder tumorigenesis by showing that the medians for the normal, benign tumor, T1 and T2-4 samples were 29 (n = 21; 47.6% of the values above the median), 7 (n = 31; 51.6% above the median), 35 (n = 20; 55% above the median), and 98 (n = 45; 55.5% above the median), respectively. Contrary to the breast and bladder carcinomas, analysis of Affymetrix microarray data on 118 colon biopsies (29) originating from sporadic microsatellite unstable tumors (n = 19), hereditary microsatellite unstable tumors (n = 15), or microsatellite stable tumors (n = 67) showed no significant differences in LEDGF expression levels when compared with normal colon (n = 17).

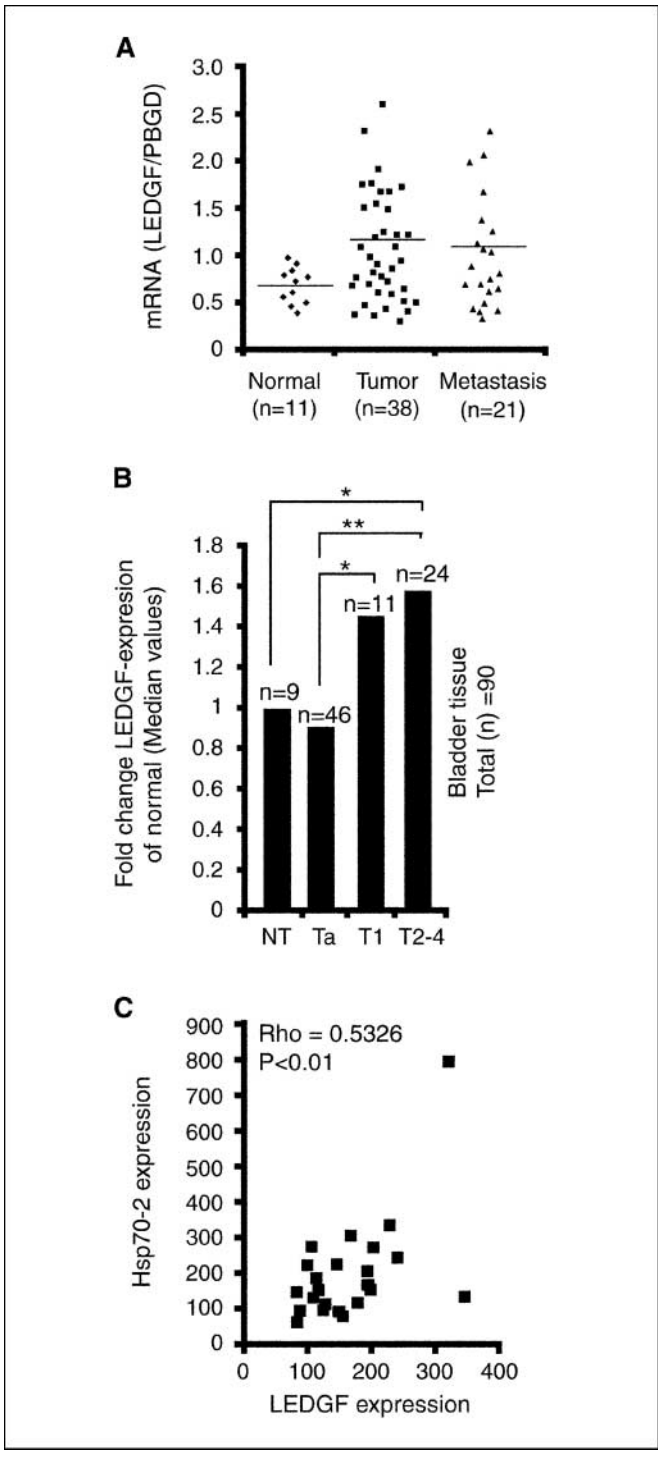

Figure 6. The expression of LEDGF mRNA is up-regulated in breast and bladder cancer. *A,* LEDGF mRNA expression levels in human mammary biopsies originating from normal, primary tumor or metastatic tumor samples were determined by real-time RT-PCR. Each dot represents an independent tissue sample where LEDGF levels are depicted relative to PBGD levels. *Horizontal lines,* median values. $P > 0.05$. *B,* median values of LEDGF expression in 90 samples of bladder tissue sorted according to pathologic definitions as normal epithelium (*NT*), benign tumor (*Ta*), subepithelium/connective tissue–invasive carcinoma (*T1*), and muscle-invasive carcinoma (*T2-4*). *, P value <0.05; **, P value <0.01. *C,* comparison of LEDGF and Hsp70-2 mRNA expression in 9 samples of normal bladder tissue and 24 samples of muscle-invasive bladder cancer. The significance of correlation was analyzed by Pearson's product moment test: Rho = 0.5326; P value <0.01.

Discussion

Transformation and tumor environment enhance the expression of lysosomal cysteine cathepsins and increase their secretion into the extracellular space (37–40). These changes lead not only to cathepsin-mediated increase in angiogenesis, tumor growth, and metastatic capacity, but also to an increased susceptibility to lysosomal destabilization and cathepsin-dependent cell death. Accordingly, tumor progression has been suggested to require cellular changes that confer resistance not only to apoptosis but also

to lysosomal cell death pathways (14, 15, 18). The data presented above identify LEDGF as an Hsp70-2–regulated protein that can mediate such changes by stabilizing the lysosomes and thereby enhancing tumor cell survival both *in vitro* and *in vivo*. Thus, both LEDGF and Hsp70-2 emerge as potential targets for therapy of invasive cancers with acquired defects in their apoptosis signaling.

We have earlier shown that Hsp70-2 depletion results in a substantial up-regulation of MIC-1 expression and MIC-1–dependent growth arrest specifically in cancer cells (10). The data presented here reveal an additional tumorigenic effect of Hsp70-2, i.e., positive regulation of LEDGF expression and LEDGF-mediated enhanced survival potential. Akin to the MIC-1 regulation, the transcriptional control of LEDGF is specific to Hsp70-2 because the depletion of highly related cytosolic Hsp70 members failed to down-regulate LEDGF mRNA levels. The two responses are, however, controlled differently. Whereas the regulation of MIC-1 expression is limited to cancer cells, Hsp70-2 regulates LEDGF levels also in immortalized epithelial cells. The up-regulation of MIC-1 that is limited to Hsp70-2–depleted cancer cells may thus be part of a stress response created by the absence of Hsp70-2, whereas the Hsp70-2–mediated positive control of LEDGF could reflect a more direct role for Hsp70-2 in the transcriptional regulation. This idea is supported by the data showing that both up- and down-regulation of Hsp70-2 affect LEDGF expression in cultured cells, and that expression of Hsp70-2 and LEDGF show a significant positive correlation in bladder biopsies.

Interestingly, our data show that LEDGF (and Hsp70-2) controls a lysosomal cell death pathway rather than caspase-mediated apoptosis: (*a*) the cancer cell death associated with the LEDGF depletion was not accompanied by detectable caspase activation, but was instead preceded by an increase in the volume of the acidic compartment of the cell, increased number of autophagosomes, and the leakage of the lysosomal proteases into the cytosol; (*b*) pharmacologic inhibition of cathepsin B, but not that of caspases, conferred significant protection against cell death induced by LEDGF siRNAs; (*c*) the antiapoptotic Bcl-2 failed to rescue the LEDGF-depleted cells from cell death; and finally (*d*) ectopic LEDGF stabilized the lysosomal membranes and conferred protection against agents known to trigger the lysosomal cell death pathway. Of special interest is the ability of LEDGF to confer protection to the sigma-2 receptor ligand that kills cancer cells by direct destabilization of the lysosomes in a Bcl-2–insensitive manner (24).[3] Consistent with our data, LEDGF protects lens epithelial cells against a nonapoptotic and Bcl-2–insensitive cell death induced by H_2O_2, a potent inducer of lysosomal leakage (33, 34, 41, 42). In addition to the oxidative stress, LEDGF enhances the survival of various benign cell types under other stress conditions, including heat, alcohol, and starvation (33, 34). Interestingly, the death induced by the LEDGF depletion under normal culture conditions was observed only in cancer cells, primary fibroblasts, and immortalized epithelial cells not being affected. These data suggest that cancer cells may be challenged by a constitutive stress signaling that affects their lysosomal compartment and renders them especially vulnerable to additional destabilization of lysosomes. It should be noted that only four nontumorigenic and three cancer cell lines were tested in this study, and the difference observed between nontumorigenic and cancer-derived cell lines could also reflect other differences between the cell lines than their transformation status.

[3] Unpublished data.

LEDGF is a weak transcriptional coactivator that interacts with various transcriptional activators and components of the basal transcriptional machinery (43). Furthermore, it binds to heat shock elements and stress response elements, thereby activating transcription of various Hsps (particularly Hsp27, αβ-crystallin, and Hsp90) and other stress-related proteins (e.g., antioxidant protein 2; refs. 33, 34). The above-mentioned target genes have been suggested to mediate the prosurvival effect of LEDGF in lens epithelial cells. It remains to be studied whether the LEDGF-mediated stabilization of cancer cell lysosomes and the associated enhancement of cancer cell survival and tumor growth observed in this study depend on LEDGF's transcriptional activity. It should, however, be noted that none of the suggested LEDGF targets or known lysosomal proteins are among the 90 genes in which expression is down-regulated together with LEDGF in Hsp70-2–depleted HeLa cells (10). Furthermore, our preliminary experiments failed to recognize consistent changes in the expression levels of heat shock element–regulated Hsps (Hsp70-1 and Hsp27), lysosomal membrane proteins (LAMP-1 and LAMP-2), or cysteine cathepsins (B and L) in cells transfected with either LEDGF cDNA or siRNA (data not shown). Alternatively, LEDGF could have a direct stabilizing effect on the lysosomes. Immunoblot analysis failed, however, to detect any LEDGF in lysosomes isolated either from untreated or stressed MCF-7 cells (data not shown).

Consistent with our data showing that LEDGF mRNA expression is elevated in breast and bladder cancers, LEDGF was recently identified as a tumor-associated antigen in the adenocarcinoma of prostate (44). A tissue array analysis of 56 prostate cancer samples revealed strong LEDGF staining in 61% of the samples, whereas three samples originating from normal prostate were negative. Akin to our bladder cancer material, a histologic analysis of the prostate cancer samples showed a tendency for increased LEDGF staining correlating with advanced tumor stage. Of further interest to the cancer field is that the *LEDGF* gene is localized to chromosome 9p22.2 and is involved in a t(9;11)(p22;p15) recurrent but rare translocation in acute and chronic myeloid leukemias (45–48). Although it is not clear how this translocation leads to leukemia, one possibility is that it enhances the transcriptional activation by *LEDGF*. In the leukemia-related translocations, the COOH terminus of the *LEDGF* is fused to the NH_2 terminus of the nucleoprotein-98 gene. Such a fusion can result in the replacement of the NH_2-terminal *LEDGF* sequences that act as transcriptional repressors with FXFG repeats of nucleoprotein-98 that possess strong transcriptional activation activity (45, 49).

In conclusion, our data define novel functions for Hsp70-2 and LEDGF in the control of the stability of cancer lysosomes. These data open exciting possibilities for the development of cancer therapies based on the inhibition of either expression or function of these proteins.

Acknowledgments

Received 11/7/2006; revised 12/29/2006; accepted 1/10/2007.

Grant support: Danish Cancer Society (M. Jäättelä), the Danish National Research Foundation (M. Jäättelä), the Danish Medical Research Council (M. Jäättelä), the Meyer Foundation (M. Jäättelä), the Novo Nordisk Foundation (M. Rohde), and the Association for International Cancer Research (M. Jäättelä).

The costs of publication of this article were defrayed in part by the payment of page charges. This article must therefore be hereby marked *advertisement* in accordance with 18 U.S.C. Section 1734 solely to indicate this fact.

We thank Jane Hinrichsen, Karina Grøn Henriksen, and Talal Chabaan for excellent technical assistance and Anthony Cerami, Per Guldberg, Boris Margulis, Bob Rydzewski, Christian Thomsen, and Per Thor Straten for valuable reagents.

References

1. Bukau B, Weissman J, Horwich A. Molecular chaperones and protein quality control. Cell 2006;125:443–51.
2. Tavaria M, Gabriele T, Kola I, Anderson RL. A hitchhiker's guide to the human Hsp70 family. Cell Stress Chaperones 1996;1:23–8.
3. Jäättelä M. Heat shock proteins as cellular lifeguards. Ann Med 1999;31:261–71.
4. Ciocca DR, Clark GM, Tandon AK, Fuqua SA, Welch WJ, McGuire WL. Heat shock protein hsp70 in patients with axillary lymph node-negative breast cancer: prognostic implications. J Natl Cancer Inst 1993;85:570–4.
5. Jäättelä M. Over-expression of hsp70 confers tumorigenicity to mouse fibrosarcoma cells. Int J Cancer 1995; 60:689–93.
6. Wei Y, Zhao X, Kariya Y, Teshigawara K, Uchida A. Inhibition of proliferation and induction of apoptosis by abrogation of heat-shock protein (HSP) expression in tumor cells. Cancer Immunol Immunother 1995;40: 73–8.
7. Vargas-Roig LM, Gago FE, Tello O, Aznar JC, Ciocca DR. Heat shock protein expression and drug resistance in breast cancer patients treated with induction chemotherapy. Int J Cancer 1998;79:468–75.
8. Nylandsted J, Rohde M, Brand K, Bastholm L, Elling F, Jäättelä M. Selective depletion of heat shock protein 70 (Hsp70) activates a tumor-specific death program that is independent of caspases and bypasses Bcl-2. Proc Natl Acad Sci U S A 2000;97:7871–6.
9. Xanthoudakis S, Nicholson DW. Heat-shock proteins as death determinants. Nat Cell Biol 2000;2:E163–5.
10. Rohde M, Daugaard M, Jensen MH, Helin K, Nylandsted J, Jäättelä M. Members of the heat-shock protein 70 family promote cancer cell growth by distinct mechanisms. Genes Dev 2005;19:570–82.
11. Son WY, Hwang SH, Han CT, Lee JH, Kim S, Kim YC. Specific expression of heat shock protein HspA2 in human male germ cells. Mol Hum Reprod 1999;5:1122–6.
12. Zhu D, Dix DJ, Eddy EM. HSP70-2 is required for CDC2 kinase activity in meiosis I of mouse spermatocytes. Development 1997;124:3007–14.
13. Dix DJ, Allen JW, Collins BW, et al. Targeted gene disruption of Hsp70-2 results in failed meiosis, germ cell apoptosis, and male infertility. Proc Natl Acad Sci U S A 1996;93:3264–8.
14. Hanahan D, Weinberg RA. The hallmarks of cancer. Cell 2000;100:57–70.
15. Jäättelä M. Multiple cell death pathways as regulators of tumour initiation and progression. Oncogene 2004;23: 2746–56.
16. Brunk UT, Neuzil J, Eaton JW. Lysosomal involvement in apoptosis. Redox Rep 2001;6:91–7.
17. Leist M, Jäättelä M. Four deaths and a funeral: from caspases to alternative mechanisms. Nat Rev Mol Cell Biol 2001;2:589–98.
18. Kroemer G, Jäättelä M. Lysosomes and autophagy in cell death control. Nat Rev Cancer 2005;5:886–97.
19. Kato H. Expression and function of squamous cell carcinoma antigen. Anticancer Res 1996;16:2149–53.
20. Kuopio T, Kankaanranta A, Jalava P, et al. Cysteine proteinase inhibitor cystatin A in breast cancer. Cancer Res 1998;58:432–6.
21. Medema JP, de Jong J, Peltenburg LT, et al. Blockade of the granzyme B/perforin pathway through overexpression of the serine protease inhibitor PI-9/SPI-6 constitutes a mechanism for immune escape by tumors. Proc Natl Acad Sci U S A 2001;98:11515–20.
22. Nylandsted J, Gyrd-Hansen M, Danielewich A, et al. Hsp70 promotes cell survival by inhibiting lysosomal membrane permeabilization. J Exp Med 2004;200:425–35.
23. Bivik C, Rosdahl I, Ollinger K. Hsp70 protects against UVB induced apoptosis by preventing release of cathepsins and cytochrome *c* in human melanocytes. Carcinogenesis 2006. E-pub ahead of print.
24. Ostenfeld MS, Fehrenbacher N, Høyer-Hansen M, Thomsen C, Farkas T, Jäättelä M. Effective tumor cell death by sigma-2 receptor ligand siramesine involves lysosomal leakage and oxidative stress. Cancer Res 2005; 65:8975–83.
25. Høyer-Hansen M, Bastholm L, Szyniarowski P, et al. Control of macroautophagy by calcium, calmodulin-dependent kinase kinase β and Bcl-2. Mol Cell 2007; 25: 193–205.
26. Aaboe M, Birkenkamp-Demtroder K, Wiuf C, et al. SOX4 expression in bladder carcinoma: clinical aspects and *in vitro* functional characterization. Cancer Res 2006;66:3434–42.
27. Aaboe M, Marcussen N, Jensen KM, Thykjaer T, Dyrskjot L, Orntoft TF. Gene expression profiling of noninvasive primary urothelial tumours using microarrays. Br J Cancer 2005;93:1182–90.
28. Dyrskjot L, Thykjaer T, Kruhoffer M, et al. Identifying distinct classes of bladder carcinoma using microarrays. Nat Genet 2003;33:90–6.
29. Kruhoffer M, Jensen JL, Laiho P, et al. Gene expression signatures for colorectal cancer microsatellite status and HNPCC. Br J Cancer 2005;92:2240–8.
30. Wu Z, Irizarry RA. Preprocessing of oligonucleotide array data. Nat Biotechnol 2004;22:656–8.
31. Dyrskjot L, Zieger K, Kruhoffer M, et al. A molecular signature in superficial bladder carcinoma predicts clinical outcome. Clin Cancer Res 2005;11:4029–36.
32. Foghsgaard L, Wissing D, Mauch D, et al. Cathepsin B acts as a dominant execution protease in tumor cell apoptosis induced by tumor necrosis factor. J Cell Biol 2001;153:999–1009.
33. Shinohara T, Singh DP, Fatma N. LEDGF, a survival factor, activates stress-related genes. Prog Retin Eye Res 2002;21:341–58.
34. Ganapathy V, Daniels T, Casiano CA. LEDGF/p75: a novel nuclear autoantigen at the crossroads of cell survival and apoptosis. Autoimmun Rev 2003;2:290–7.
35. Ono K, Kim SO, Han J. Susceptibility of lysosomes to rupture is a determinant for plasma membrane disruption in tumor necrosis factor α-induced cell death. Mol Cell Biol 2003;23:665–76.
36. Andersen JB, Aaboe M, Borden EC, Goloubeva OG, Hassel BA, Orntoft TF. Stage-associated overexpression of the ubiquitin-like protein, ISG15, in bladder cancer. Br J Cancer 2006;94:1465–71.
37. Joyce JA, Baruch A, Chehade K, et al. Cathepsin cysteine proteases are effectors of invasive growth and angiogenesis during multistage tumorigenesis. Cancer Cell 2004;5:443–53.
38. Fehrenbacher N, Gyrd-Hansen M, Poulsen B, et al. Sensitization to the lysosomal cell death pathway upon immortalization and transformation. Cancer Res 2004; 64:5301–10.
39. Sloane BF, Yan S, Podgorski I, et al. Cathepsin B and tumor proteolysis: contribution of the tumor microenvironment. Semin Cancer Biol 2005;15:149–57.
40. Gocheva V, Zeng W, Ke D, et al. Distinct roles for cysteine cathepsin genes in multistage tumorigenesis. Genes Dev 2006;20:543–56.
41. Brunk UT, Svensson I. Oxidative stress, growth factor starvation and Fas activation may all cause apoptosis through lysosomal leak. Redox Rep 1999;4:3–11.
42. Mao YW, Xiang H, Wang J, Korsmeyer S, Reddan J, Li DW. Human bcl-2 gene attenuates the ability of rabbit lens epithelial cells against H_2O_2-induced apoptosis through down-regulation of the α B-crystallin gene. J Biol Chem 2001;276:43435–45.
43. Ge H, Si Y, Roeder RG. Isolation of cDNAs encoding novel transcription coactivators p52 and p75 reveals an alternate regulatory mechanism of transcriptional activation. EMBO J 1998;17:6723–9.
44. Daniels T, Zhang J, Gutierrez I, et al. Antinuclear autoantibodies in prostate cancer: immunity to LEDGF/p75, a survival protein highly expressed in prostate tumors and cleaved during apoptosis. Prostate 2005;62:14–26.
45. Ahuja HG, Hong J, Aplan PD, Tcheurekdjian L, Forman SJ, Slovak ML. t(9;11)(p22;p15) in acute myeloid leukemia results in a fusion between NUP98 and the gene encoding transcriptional coactivators p52 and p75-lens epithelium-derived growth factor (LEDGF). Cancer Res 2000;60:6227–9.
46. Hussey DJ, Moore S, Nicola M, Dobrovic A. Fusion of the NUP98 gene with the LEDGF/p52 gene defines a recurrent acute myeloid leukemia translocation. BMC Genet 2001;2:20.
47. Grand FH, Koduru P, Cross NC, Allen SL. NUP98-LEDGF fusion and t(9;11) in transformed chronic myeloid leukemia. Leuk Res 2005;29:1469–72.
48. Morerio C, Acquila M, Rosanda C, et al. t(9;11)(p22;p15) with NUP98-LEDGF fusion gene in pediatric acute myeloid leukemia. Leuk Res 2005;29:467–70.
49. Singh DP, Kubo E, Takamura Y, et al. DNA binding domains and nuclear localization signal of LEDGF: contribution of two helix-turn-helix (HTH)-like domains and a stretch of 58 amino acids of the N-terminal to the trans-activation potential of LEDGF. J Mol Biol 2006;355: 379–94.